Scientific Journal for Damietta Faculty of Science **15**(1) 2025, 111-**117**
Doi: 10.21608/sjdfs.2025.353366.1214
ISSN Print 2314-8594
ISSN Online 2314-8616

https://sjdfs.journals.ekb.eg/

The Changes in the Nonlinear Properties of Chitosan Induced by Chemical Modification

Hajer Abusnina[*1,2],N. A. El-Ghamaz[1] and E. A. Gaml[1]

[1]Department of Physics, Faculty of Science, Damietta University 34517, Egypt.
[2]High and Intermediate Institute of Agricultural Technology-Gheran. Tripoli, Libya.

Received: 15 January 2025 /Accepted: 09 February 2025

[*]Corresponding author's E-mail: hajer.gege2014@gmail.com

Abstract

A spin coating was used to prepare thin films of Chitosan and its derivative. Fourier Transform Infrared (FTIR) spectroscopy was adopted to identification of chemical bonds and functional groups of Chitosan and its derivative. The optical properties of thin films were investigated using the spectrophotometric measurements of the transmittance, T(λ), and reflectance, R(λ), at normal incidence of light in the wavelength range 200 - 2500 nm. The complex refractive index (n^*) and complex dielectric constant (ε^*), as well as, the nonlinear optical properties (third order nonlinear susceptibility and the nonlinear refractive index) of Chitosan and its derivative was determined and analyzed.

Keywords: Spin coting; complex refractive index; complex dielectric constant; Nonlinear third order nonlinear susceptibility.

Introduction

Polymeric composites have garnered significant interest due to their remarkable applicability across diverse sectors, encompassing industrial, biological, medical, shielding, and entertainment domains (Prabaharan, 2015). Chitosan is a natural and renewable biopolymer which has been derived from Chitin, the Earth's second most abundant natural polymer. Obtained through alkali-mediated deacetylation, Chitosan exhibits several advantageous properties such as biocompatibility, solubility in aqueous media, biodegradability, thermal stability, chemical resistance, and non-toxicity (Aziz et al., 2017).

Chitosan is a biodegradable, safe, antibacterial, and biocompatible polymer. It finds applications in various medical and industrial fields. In healthcare, it is utilized as a dressing material for burn and wound care due to its advantageous properties (Siddiqui et al., 2017; Wu et al., 2006). Applications based on the optical properties of Chitosan are emerging. For instance, the development of sensors to detect metal ions and biological structures, based on resonant excitation of surface free-electrons oscillations has been considered

(Sugunan et al., 2005). (Fernandes Queiroz et al., 2014) found that the FTIR data show that the Chitosan exhibited the function group and characteristic signals of the polymers. Nonlinear optics investigates the behavior of powerful light beams passing through materials. These intense light beams can alter the material's optical characteristics, resulting in unique phenomena not observed in materials that respond linearly to light. These phenomena can modify polarization features or generate entirely new frequency components (Drake, 2023). Nonlinear optics study has a key role in fundamental applications of all optical signals processing units, switching devices and optical circuits (Nasher et al., 2019; P. Sharma & Katyal, 2010).

In the present work, we aimed to investigate the optical linear and nonlinear properties of Chitosan and report about the effect linkage of conjugated function group to the Chitosan backbone on its optical constants and nonlinear properties.

Experimental techniques

Material

In is work, Chitosan was used as received powder. Modified Chitosan powder was synthesized according to the procedure reported in Ref (Diab et al., 2011). The molecular structure of Chitosan and Modified Chitosan (Mod-Chitosan) are shown in Fig. 1. Since Chitosan derivative is found to be insoluble in synthesize pure form, studying its optical properties is feasible when mixed with Chitosan due to its easy solubility. This resulted appearance a new composite, **Chi-MD**.

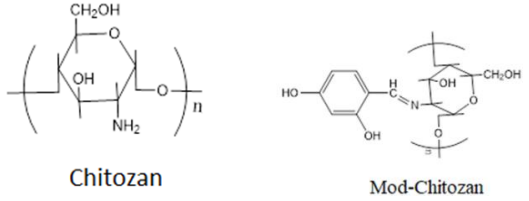

Fig.1: Scheme of the chemical structure for Chitosan and Mod-Chitosan**.**

Experimental techniques and Samples preparation:

FT-IR spectra are recorded by FT-IR (FT1IR 430-JASCO, Japan) in the wavenumber range 4000–400 cm^{-1}. The reflectance R(λ) and transmittance T (λ) for thin films of as received Chitosan and its derivative thin films are recorded by JASCO model V-570 UV- vis-NIR in the range 200-2500 nm in normal incidence of light. All measurements are performed in ambient room temperature.

To prepare the pure Chitosan solution, 0.1 g of Chitosan was dissolved in 4 mL of acetic acid solution and 2 mL of distilled water. The solution was then stirred for 12 hours at room temperature. For preparing solution of Chi-MD, the mixture of the polymers is mixed with ratio 2:1 of Chitosan to Mod-Chitosan and dissolved solvents of chitosan. The produce solution was stirred for 12 hours at room temperature to insure complete homogeneity and solubility of the mixture (Chi-MD). Thin films of Chitosan and Chi-MD were fabricated using a spin coating technique on optical flat quartz substrates. A VTC-50A Spin Coater was employed at 1500 rpm for thin film deposition and 2500 rpm for drying. Each step lasting 30 seconds.

Result and discussion

Fourier transforms infrared (FTIR) spectroscopy:

Figure 2 displays the FTIR spectra of Chitosan and its derivative. The standard absorption peaks that characterize the Chitosan are presented in the IR charts of Chitosan and its derivative Mod-Chitosan. The FTIR spectrum of Chitosan shows a broad band at 3289 cm^{-1} due to OH and NH_2 groups (Sajomsang et al., 2009)**.** Also, in Mod-Chitosan, new absorption peaks appeared, some disappeared or shifted due to the addition of substituent group to Chitosan molecule (Lawrie et al., 2007). The peak at 2213 cm^{-1} in Chitosan polymer corresponds to C=N, and shifted to 2270 and 2272 cm^{-1} for polymer Mod-Chitosan as an effect of coupling with the aromatic group. The bands at 1655 and 1322 cm^{-1} are assigned to the amino group while the bands at 1424 and 1379 cm^{-1} are assigned to O-C-O group (Diab et al., 2011). There are some absorption peaks observed only for polymers Mod-Chitosan due to the substitution reaction. Polymer is characterized by the peaks at 1630 and 1660 cm^{-1}, respectively, which are assigned to C=C stretching of the substituted phenyl ring

(Osman & Arof, 2003). Also, the new absorption peaks observed in polymer Mod-Chitosan at the range 870-600 cm^{-1} can be assigned to the C-C stretching of the substituted phenyl ring (Ţucureanu et al., 2016).

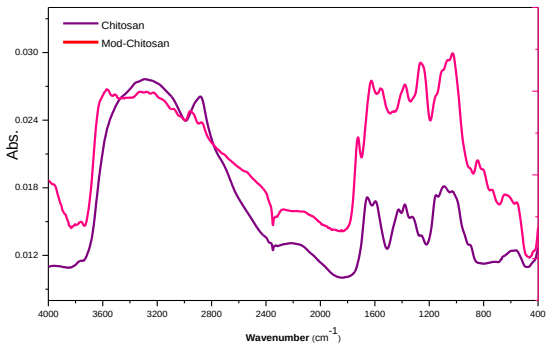

Fig 2: Fourier transform infrared spectra of Chitosan and Mod-Chitosan.

Optical characterization

The spectral behavior of transmittance, T, and reflectance, R:

Figures 3 and 4 present the transmittance (T) and reflectance (R) spectra of Chitosan and its derivative, Chi-MD, respectively, across the wavelength range of 200-2500 nm. Both materials display similar spectral behavior in the near-infrared region (700-2500 nm) with respect to transmittance and reflectance. However, significant differences are observed in both T and R spectra within the visible and ultraviolet region (200-700 nm). This distinct behavior can be attributed to the chemical modifications introduced to the Chitosan polymer (Good et al., 2016), as illustrated in Figure 1, which consequently alters the absorption and refractive properties of the material.

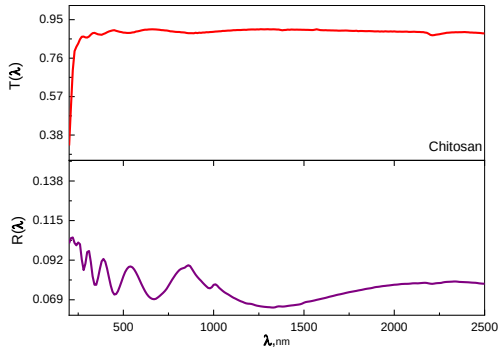

Fig 3: T and R spectra of Chitosan.

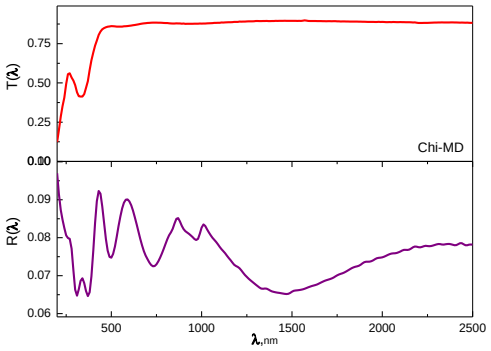

Fig 4: T and R spectra of Chi-MD.

Refractive index (n) and extinction coefficient (k)

Refractive index (n) and absorption index (k) are fundamental parameters for the design and optimization of integrated optical devices. The complex refractive index, $\tilde{n}$, is expressed by the following relation (El-Nahass & Youssef, 2010):

$$\tilde{n} = n - ik \qquad (1)$$

The real part of refractive index, n, can be determined from the absolute reflectance (R) of the material and its extinction coefficient (k) using the following relation (El-Nahass & Youssef, 2010):

$$n = \frac{(1+R)}{(1-R)} + \sqrt{\left(\left(\frac{4R}{(1-R)^2}\right) - k^2\right)} \qquad (2)$$

The spectral distribution of the calculated refractive index, n, in the wavelength range 200-2500 nm for thin films of Chitosan and Chi-MD are presented in Fig 5. The spectral behavior of the refractive index (n) for both polymers exhibits anomalous dispersion within the 200-600 nm wavelength range. This behavior is attributed to photon absorption phenomena. The multi-oscillator model (Hammond, 1997) , which considers multiple electronic transitions from bonding to antibonding molecular orbitals, can effectively explain this behavior. In contrast, normal dispersion of n is observed in the wavelength range of 600-2500 nm, which is characterized by the absence of electronic transitions and corresponds to the transparent region of the material (Zaki et al., 2022).

The extinction coefficient, or absorption index (k), represents the imaginary part of the complex refractive index and quantifies the extent to which a material absorbs

light at a specific wavelength. Figure 6 presents the spectral distribution of k for thin films of pristine Chitosan and its derivative, Chi-MD. Both materials exhibit a prominent absorption peak, albeit with a difference in peak position (Mohammed & Yahia, 2018). These absorption peaks are attributed to π-π* electronic transitions involving the excitation of electrons from bonding to antibonding molecular orbitals (Fox, 2012).

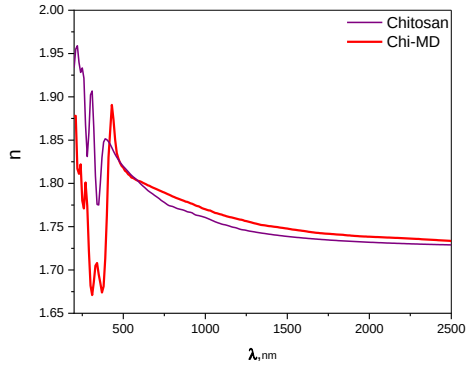

Fig 5: Spectral distribution of n of Chitosan and Chi-MD.

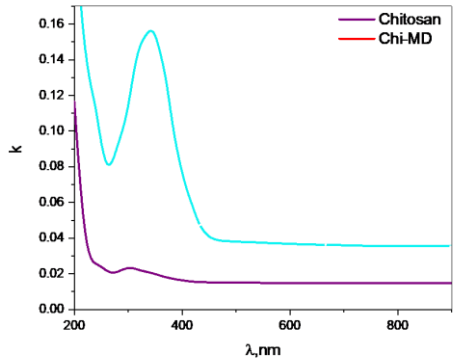

Fig 6: The spectral behaviors of the extinction coefficient, k for Chitosan and Chi-MD.

Dielectric constants

The dielectric function links a solid's electronic transitions to its structure, enabling the extraction of valuable band structure information from its dielectric spectrum (Bird, 2002).. The real component (ε_r) and the imaginary component (ε_i) of the complex dielectric constant (ε*) are interconnected by the following equations (Palik & Ghosh, 1998):

$$\varepsilon^* = \varepsilon_r - i\varepsilon_i, \quad (5)$$

where

$$\varepsilon_r = n^2 - k^2 \quad (6)$$

and

$$\varepsilon_i = 2nk\,. \quad (7)$$

The spectral characteristics of the real (ε_r) and imaginary (ε_i) components of the dielectric constant are modulated by variations in both refractive index (n) and extinction coefficient (k). Figures 7 and 8 illustrate the impact of functional group substitution on the spectral behavior of ε_r and ε_i for pristine Chitosan and its derivative, Chi-MD. Generally, ε_r values exhibit a higher magnitude compared to ε_i values for both Chitosan and its derivative. The spectral distribution of ε_r and ε_i signifies diverse interactions between incident photons and the investigated films. Peaks observed within the 200-450 nm wavelength range are attributed to electronic transitions from bonding to antibonding molecular orbitals, induced by photon absorption. The peak position is influenced by modifications to the chitosan molecule. Normal dispersion is exhibited by all samples at wavelengths up to 2500 nm. This indicates a more stable interaction with light, where the dielectric properties become less sensitive to changes in wavelength, suggesting consistent material response across a broader range of conditions.

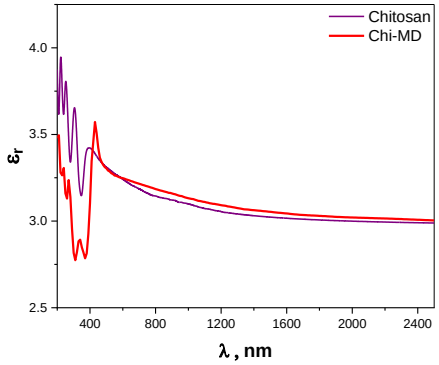

Fig 7: Spectral behavior of real dielectric constant ε_r for Chitosan and Chi-MD.

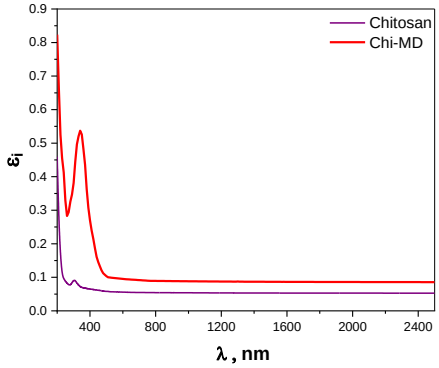

Fig 8 :Spectral behavior of imaginary dielectric constant ε_i for Chitosan and Chi-MD.

Non-linear optical parameters

Understanding nonlinear optical properties is crucial for utilizing Chitosan in modern optical technologies (Dalton, 2013). The study of these properties is essential for various optoelectronic applications. Nonlinear optical phenomena occur when materials interact with high-intensity electromagnetic fields (Shanmugavelu et al., 2013). The third-order nonlinear optical susceptibility (χ^3) and the nonlinear refractive index (n_2) are key parameters that determine a material's nonlinear optical response (Abuelwafa et al., 2015; I. Sharma et al., 2014). These parameters can be estimated using the following relations (Ticha & Tichy, L, 2004) (Wynne, 1969):

$$\chi^{(1)} = (n^2 - 1)/4\pi \quad (12)$$

$$\chi^{(3)} = A[\chi^{(1)}]^4 \quad (13)$$

$$n_2 = \frac{12\pi}{n_o}\chi^{(3)} \quad (14)$$

where, A = 1.7 x 10^{-10} esu and $n_o = \sqrt{\varepsilon_\infty}$,

The obtained results of the nonlinear optical properties $\chi^{(3)}$ and n_2 for Chitosan and Chi-MD thin films are shown in Figure 9 and 10. The results indicate that the values of $\chi^{(3)}$ and n_2 for Chi-MD showed lower values than that of Chitosan in the wavelength range 200-500 nm. On the other hand, both of $\chi^{(3)}$ and n_2 show nearly the same behavior of chitosan and Chi-MD.

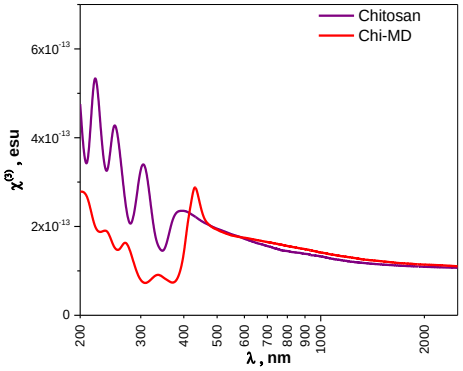

Fig 9: Plot third order nonlinear susceptibility $\chi^{(3)}$ versus incident photon energy, λ, for Chitosan and Chi-MD

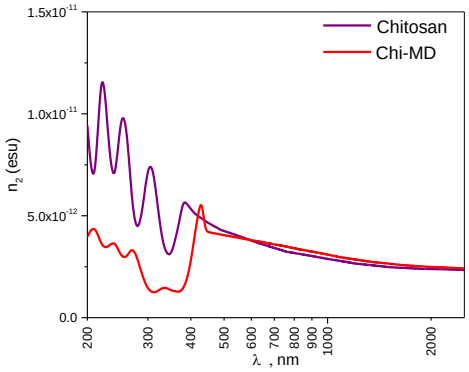

Fig 10: Plot the non-linear refractive index n_2 versus incident photon energy, λ, for Chitosan and Chi-MD

Conclusions

In this study, thin films of both Chitosan and Chi-MD were successfully fabricated using the spin-coating technique. FTIR analysis of the polymer powders confirmed the chemical structure of Chitosan and its derivative, as well as the successful coupling of the functional group via the Schiff base reaction. The spectral behavior of the refractive index (n) for both polymers exhibited anomalous dispersion within the 200-600 nm wavelength range. In contrast, normal dispersion of n was observed in the wavelength range of 600-2500 nm. Both Chitosan and Chi-MD thin films exhibited a prominent absorption peak, albeit with a difference in peak position. These absorption peaks are attributed to π-π* electronic transitions involving the excitation of electrons from bonding to antibonding molecular orbitals. The real part of the dielectric constant (ε_r) exhibited a higher magnitude compared to the imaginary part (ε_i) for both Chitosan and its derivative. Calculations of the third-order nonlinear optical susceptibility (χ^3) and the nonlinear refractive index (n_2) for Chi-MD showed lower values compared to Chitosan within the wavelength range of 200-500 nm. Conversely, both χ^3 and n_2 exhibited nearly identical behavior in the remaining wavelength range.

References

Abuelwafa, A. A., El-Denglawey, A., Dongol, M., El-Nahass, M. M., & Soga, T. (2015). Influence of annealing temperature on structural and optical properties of nanocrystalline Platinum octaethylporphyrin (PtOEP) thin films. Optical

Materials, 49, 271–278. https://doi.org/10.1016/j.optmat.2015.09.032

Aziz, S. B., Abdullah, O. Gh., Hussein, S. A., & Ahmed, H. M. (2017). Effect of PVA Blending on Structural and Ion Transport Properties of CS:AgNt-Based Polymer Electrolyte Membrane. Polymers, 9(11), 622. https://doi.org/10.3390/polym9110622

Bird, J. P. (2002). Semiconductors: An Introduction. In Encyclopedia of Materials: Science and Technology (pp. 1–16). Elsevier. https://doi.org/10.1016/B0-08-043152-6/01854-4

Dalton, L. R. (2013). Polymers for Nonlinear Optics. In S. Kobayashi & K. Müllen (Eds.), Encyclopedia of Polymeric Nanomaterials (pp. 1–6). Springer Berlin Heidelberg. https://doi.org/10.1007/978-3-642-36199-9_11-1

Diab, M. A., El-Sonbati, A. Z., & Bader, D. M. D. (2011). Thermal stability and degradation of chitosan modified by benzophenone. Spectrochimica Acta Part A: Molecular and Biomolecular Spectroscopy, 79(5), 1057–1062. https://doi.org/10.1016/j.saa.2011.04.019

Drake, G. W. F. (Ed.). (2023). Springer Handbook of Atomic, Molecular, and Optical Physics. Springer International Publishing. https://doi.org/10.1007/978-3-030-73893-8

El-Nahass, M. M., & Youssef, T. E. (2010). Influence of X-ray irradiation on the optical properties of ruthenium(II)octa-(n-hexyl)-phthalocyanine thin film. Journal of Alloys and Compounds, 503(1), 86–91. https://doi.org/10.1016/j.jallcom.2010.04.029

Fernandes Queiroz, M., Melo, K., Sabry, D., Sassaki, G., & Rocha, H. (2014). Does the Use of Chitosan Contribute to Oxalate Kidney Stone Formation? Marine Drugs, 13(1), 141–158. https://doi.org/10.3390/md13010141

Fox, M. (2012). Optical properties of solids (2. ed., reprinted). Oxford Univ. Press.

Good, P., Cooper, T., Querci, M., Wiik, N., Ambrosetti, G., & Steinfeld, A. (2016). Spectral reflectance, transmittance, and angular scattering of materials for solar concentrators. Solar Energy Materials and Solar Cells, 144, 509–522. https://doi.org/10.1016/j.solmat.2015.09.057

Hammond, C. (1997). The basics of crystallography and diffraction. Oxford University Press.

Lawrie, G., Keen, I., Drew, B., Chandler-Temple, A., Rintoul, L., Fredericks, P., & Grøndahl, L. (2007). Interactions between Alginate and Chitosan Biopolymers Characterized Using FTIR and XPS. Biomacromolecules, 8(8), 2533–2541. https://doi.org/10.1021/bm070014y

Mohammed, M. I., & Yahia, I. S. (2018). Synthesis and optical properties of basic fuchsin dye-doped PMMA polymeric films for laser applications: Wide scale absorption band. Optical and Quantum Electronics, 50(3), 159. https://doi.org/10.1007/s11082-018-1425-0

Nasher, M. A., Youssif, M. I., El-Ghamaz, N. A., & Zeyada, H. M. (2019). Linear and nonlinear optical properties of irradiated Toluidine Blue thin films. Optik, 178, 532–543. https://doi.org/10.1016/j.ijleo.2018.10.001

Osman, Z., & Arof, A. K. (2003). FTIR studies of chitosan acetate based polymer electrolytes. Electrochimica Acta, 48(8), 993–999. https://doi.org/10.1016/S0013-4686(02)00812-5

Palik, E. D., & Ghosh, G. (Eds.). (1998). Handbook of optical constants of solids. Academic Press.

Prabaharan, M. (2015). Chitosan-based nanoparticles for tumor-targeted drug delivery. International Journal of Biological Macromolecules, 72, 1313–1322. https://doi.org/10.1016/j.ijbiomac.2014.10.052

Sajomsang, W., Gonil, P., & Saesoo, S. (2009). Synthesis and antibacterial activity of methylated N-(4-N,N-dimethylaminocinnamyl) chitosan chloride. European Polymer Journal, 45(8), 2319–2328. https://doi.org/10.1016/j.eurpolymj.2009.05.009

Shanmugavelu, B., Ravi Kanth Kumar, V. V., Kuladeep, R., & Narayana Rao, D. (2013). Third order nonlinear optical properties of bismuth zinc borate glasses. Journal of Applied Physics, 114(24), 243103. https://doi.org/10.1063/1.4858422

Sharma, I., Tripathi, S. K., & Barman, P. B. (2014). Thickness-dependent optical properties and nonlinear refractive index of a -Ge–Se–In thin films. Phase Transitions, 87(4), 363–375. https://doi.org/10.1080/01411594.2013.820828

Sharma, P., & Katyal, S. C. (2010). Linear and nonlinear refractive index of As–Se–Ge and Bi doped As–Se–Ge thin films. Journal of Applied Physics, 107(11), 113527. https://doi.org/10.1063/1.3428441

Siddiqui, M. R., AlOthman, Z. A., & Rahman, N. (2017). Analytical techniques in pharmaceutical analysis: A review. Arabian Journal of Chemistry, 10, S1409–S1421. https://doi.org/10.1016/j.arabjc.2013.04.016

Sugunan, A., Thanachayanont, C., Dutta, J., & Hilborn, J. G. (2005). Heavy-metal ion sensors using chitosan-capped gold nanoparticles. Science and Technology of Advanced Materials, 6(3–4), 335–340. https://doi.org/10.1016/j.stam.2005.03.007

Ticha, H., & Tichy, L, A. J. (2004). Semiempirical relation between non-linear susceptibility (refractive index), linear refractive index and optical. Chemical Reviews, 104(12),

6017–6084. https://doi.org/00

Ţucureanu, V., Matei, A., & Avram, A. M. (2016). FTIR Spectroscopy for Carbon Family Study. Critical Reviews in Analytical Chemistry, 46(6), 502–520. https://doi.org/10.1080/10408347.2016.1157013

Wu, Y., Guo, J., Yang, W., Wang, C., & Fu, S. (2006). Preparation and characterization of chitosan–poly(acrylic acid) polymer magnetic microspheres. Polymer, 47(15), 5287–5294. https://doi.org/10.1016/j.polymer.2006.05.017

Wynne, J. J. (1969). Optical Third-Order Mixing in GaAs, Ge, Si, and InAs. Physical Review, 178(3), 1295–1303. https://doi.org/10.1103/PhysRev.178.1295

Zaki, A. A., Khalafalla, M., Alharbi, K. H., & Khalil, K. D. (2022). Synthesis, characterization and optical properties of chitosan–La2O3 nanocomposite. Bulletin of Materials Science, 45(3), 128. https://doi.org/10.1007/s12034-022-02697-2.

الملخص العربي

عنوان البحث: التغيرات في الخواص البصرية اللاخطية للكيتوزان الناجمة عن التعديل الكيميائي

هاجر عاشور محمد أبوسنينة*[1]، ناصر عبده عبدالرازق الغماز[1]، إيمان أسعد جمل[1]

[1]قسم الفيزياء – كلية العلوم – جامعة دمياط – مصر.

في هذه الدراسة، تم تحضير أفلام رقيقة من كلا من الكيتوزان و Chi-MD بنجاح باستخدام تقنية الطلاء المغزلي. أكدت تحاليل FTIRلمساحيق البوليمر على التركيب الكيميائي للكيتوزان والبوليمر المشتق منه، كما أكدت على نجاح اقتران المجموعة الوظيفية. أظهر السلوك الطيفي للمؤشر الانكساري (n) لكلا البوليمرين تشتتاً شاذًا في نطاق الطول الموجي ٢٠٠-٦٠٠ نانومتر. في المقابل، لوحظ تشتت طبيعي لـ n في نطاق الطول الموجي ٦٠٠-٢٥٠٠ نانومتر. كما أظهر كلا من أفلام الكيتوزان و Chi-MD الرقيقة ذروة امتصاص بارزة، وإن كان هناك اختلاف في موضع الذروة. تُعزى قمم الامتصاص هذه إلى انتقالات إلكترونية *π-π التي تنطوي على إثارة الإلكترونات من المدارات الجزيئية الرابطة إلى المدارات الجزيئية المضادة للرابطة. أظهر الجزء الحقيقي من الثابت الكهربائي (ε_r) مقدارًا أعلى مقارنة بالجزء التخيلي (ε_i) لكلا من الكيتوزان والبوليمر المشتق منه. كما أظهرت حسابات الاستقطاب الضوئي اللاخطي من الدرجة الثالثة (χ^3) والمؤشر الانكساري اللاخطي (n_2) لـ Chi-MD قيمًا أقل مقارنة بالكيتوزان في نطاق الطول الموجي ٢٠٠-٥٠٠ نانومتر. على العكس من ذلك، أظهر كل من χ^3 و n_2 سلوكًا متطابقًا تقريبًا في نطاق الطول الموجي من ٥٠٠ وحتى ٢٥٠٠ نانومتر.